Original Article

Evaluation of the Possible Synergic Regenerative Effects of Platelet-Rich Plasma and Hydroxyapatite/Zirconia in the Rabbit Mandible Defect Model

Sheila Shahsavari-Pour[1], MSc;
Ehsan Aliabadi[1], MSc;
Mona Latifi[2], PhD;
Nehle Zareifard[3], PhD;
Mohammad Reza Namavar[4], PhD;
Tahereh Talaei-Khozani[5], PhD

[1]Department of Oral and Maxillofacial Surgery, School of Dentistry, Shiraz University of Medical Sciences, Shiraz Iran;
[2]Department of Tissue Engineering, National Institute of Genetic Engineering and Biotechnology, Iran;
[3]Stem Cell Lab, Department of Anatomy, School of Medicine, Shiraz University of Medical Sciences, Shiraz, Iran;
[4]Department of Anatomy, School of Medicine, Shiraz University of Medical Sciences, Shiraz, Iran;
[5]Tissue Engineering Lab, Department of Anatomy, School of Medicine, Shiraz University of Medical Sciences, Shiraz, Iran

Correspondence:
Tahereh Talaei-Khozani, PhD;
Tissue Engineering Lab, Department of Anatomy, School of Medicine, Shiraz University of Medical Sciences, Zand Street, Shiraz Iran
Tel/Fax: +98 71 32304372
Email: talaeit@sums.ac.ir
Received: 15 April 2017
Revised: 6 May 2017
Accepted: 14 May 2017

What's Known

- Platelet-rich plasma and hydroxyapatite exert beneficial effects on bone repair.
- Zirconia also has beneficial effects on bone repair and improves the mechanical strength of the scaffold for bone tissue engineering.

What's New

- Combination of platelet-rich plasma/ hydroxyapatite/ zirconia provides a superior osteoconductive environment for bone repair in the short term.
- In the long term, the platelet-rich plasma/hydroxyapatite/zirconia scaffold showed no significant synergic regenerative effects in the rabbit mandible defect.

Abstract

Background: Platelet-rich plasma (PRP) and bioceramics such as hydroxyapatite (HA) and zirconium oxide (ZrO_2) are used to reconstruct mandibular defects. We sought to determine the synergistic effects of HA/ZrO_2 and PRP and compare their osteogenic activity.

Methods: ZrO_2 scaffolds were constructed by the slurry method and were then coated with HA and impregnated by PRP/ heparan sulfate (HS). Bilateral mandibular defects were created in 26 male rabbits. In 20 rabbits, the left defects were treated with $HA/ZrO_2/PRP$ (Group 1) and the corresponding right defects were filled with HA/ZrO_2 (Group 2). The 6 remaining models were treated with PRP gels at both sides (Group 3). The osteoconductivity of $HA/ZrO_2/PRP$ was compared with that of HA/ZrO_2 or PRP by radiological and histological methods after the follow-up period, at weeks 2, 6 and 8. The statistical analyses were performed by ANOVA and LSD using SPSS, version 16.0, for Windows (P<0.05).

Results: After 2 weeks, the percentage of the surface occupied by bone was significantly higher in the $HA/ZrO_2/PRP$-treated defects than in the PRP-treated defects (P=0.007). Osteoblast and osteocyte counts were higher significantly in the PRP-treated group (P=0.032); however, the cells had not started matrix formation on a large scale and just small islands of osteoid with trapped osteocytes were observed. In the long term, the regenerative potential of all the scaffolds was the same.

Conclusion: HA/ZrO_2 showed a superior osteoconductive capacity over PRP in the short term; however, they showed no long-term synergic effects.

Introduction

Ablative surgery of the mandible due to maxillofacial disorders leads to large defects, which can be reconstructed by autogenous grafts and alloplastic materials; however, each one has particular advantages and disadvantages.[1] Autologous graft surgery

has some disadvantages such as hematoma, residual pain, and esthetic problems. Also, the mandible reconstructed with autogenous grafts is not esthetically satisfying,[2] hence the need for the application of a better reconstruction method such as engineered bone replacement.

Biomimetic bone scaffolds recapitulate an appropriate base for cell attachment, proliferation, and differentiation.[3] Bioactive ceramics such as hydroxyapatite (HA) are helpful in the restoration of the bone with satisfying osteoinduction, osteocompatibility, and osteoconduction properties[3,4] without triggering a considerable immune response.[5] The biologic similarity of these ceramics with the body's mineral tissues has made them a useful bone replacement biomaterial in orthopedics and dentistry.[6] Nonetheless, porous HA is weak and is not concordant with the mechanical properties of the cortical bone in load-bearing situations; it is, therefore, feasible to combine the bioactivity of HA with the mechanical properties of bio-inert ceramics such as zirconium oxide (ZrO_2).[7] ZrO_2 with adequate bioactivity, biocompatibility, mechanical strength, and toughness can be widely used in orthopedic grafts.[8] Despite such advantages, however, ZrO_2 usually generates a flat surface not suitable for cell attachment, which affects the osteointegration of the graft.[9]

Platelet-rich plasma (PRP) contains fibrin and growth factors (GFs) and exerts beneficial effects on bone growth.[10,11] PRP provides a gel with bioactivity, integrity, and osteogenic potential.[11,12] Since osteoblasts are immobile cells, there is a tendency to use osteoconductive biomaterials such as fibrin to increase their motility.[13] On the other hand, some GFs present in PRP motivate proliferation, migration, and osteoblast differentiation among mesenchymal cells.[14] The beneficial effects of PRP on the migration of human osteoblasts have been reported previously.[15]

Bone formation is a lengthy process that requires the constant presence of GFs at its site. Most GFs such as transforming growth factor-β (TGF-β), with the ability to bond heparan sulfate (HS), play a crucial role in osteogenesis.[16] HS along with HA is used to sequester GFs and protect them from local protease; therefore, GFs permeate gradually and persist longer in the composite.[17] In addition, HS has some interactions with bone morphogenetic protein antagonists, which blocks the inhibitory effects of these agents and leads to an even higher rate of bone formation.[18]

Various studies have examined different types of materials as bone replacement such as the powder derived from demineralized bone,

HA, and other forms of allografts in combination with PRP. Nonetheless, the addition of PRP to HA/ZrO_2 composites has not been investigated yet. Moreover, there are contradictory results regarding the synergistic effects of a combination of bioceramics and PRP.[19,20]

The objectives of the present study were to determine whether the combination of HA/ZrO_2 with PRP and HS could exert a synergistic impact on bone regeneration and to compare the in vivo bone regeneration capacity of the HA/ZrO_2 scaffold with or without PRP.

Materials and Methods

Ethical Statement

This study was approved by the Ethics Committee of Shiraz University of Medical Sciences and conducted according to the ethical principles of animal handling and treatment.

Fabricating the HA/ZrO_2 Composite

The HA/ZrO_2 composite was prepared by adding 100 g of ZrO_2 (US Research Nanomaterial, USA) and 6 g of triethyl phosphate (Sigma, USA) to distilled water and mixing them for 24 hours. Subsequently, 15 g of polyvinyl butyl (Sigma Aldrich, USA) was added as a binder. Polyurethane foam was immersed into the slurry and desiccated at 80 °C for 10 minutes. After 4 cycles of immersion/desiccation, the foam was heated again at 800 °C for 5 hours at a heating rate of 2 °C/min. It was ultimately heated at 1400 °C for 3 hours.

HA and ZrO_2 interaction was prevented by dispersing 15 g of homemade fluorapatite, 1 g of triethyl phosphate, and 6 g of polyvinyl butyl in distilled water and mixing for 24 hours. The ZrO_2 scaffold was immersed in the fluorapatite slurry twice and dried at 90 °C for 20 minutes. The scaffold was heated at 800 °C for 5 hours, followed by another 3 hours at 1250 °C at the rate of 2 °C/min. Thereafter, a layer of HA was applied on the fluorapatite-coated ZrO_2 latticework through the same method. The scaffolds prepared were 9 mm in length, 5 mm in width, and 4 mm in thickness.

Loading PRP/HS

Ten mL of the rabbit blood was transferred to a tube containing citric acid and centrifuged at 5000 rpm for 15 minutes. The plasma and the buffy coat were centrifuged again at 2000 rpm for 10 minutes, and the bottom one-third was preserved in the freezer as PRP. The PRP gel was fortified with 2.5% $CaCl_2$ and immediately mixed with HS just prior to impregnation within the pores of the HA/ZrO_2 scaffold in a vacuum oven at 37 °C.

Scanning Electron Microscopy (SEM)

The scaffolds were fixed with 4% paraformaldehyde, dehydrated with gradually increasing concentrations of ethanol, and then dried by immersion in hexamethyldisilazane. The hexamethyldisilazane was allowed to evaporate and the samples were exposed to gold with a sputter coating machine (Ted Pella, Inc., USA).

Study Design and Surgical Procedure

Twenty-six male rabbits in normal health condition were selected randomly and anesthetized with an intramuscular injection of 10 mg/kg of ketamine (Alfasan, Holland) and 2 mg/kg of xylazine (Alfasan, Holland). The rabbits' mandibles were shaved and prepped. Next, via a submandibular incision, the myocutaneous flap was reflected. After muscle and periosteal retraction, a rectangular defect was applied in the body of the mandible with a fissure burr on each side (figure 1A). The left side was filled with $HA/ZrO_2/PRP$ and the right side with HA/ZrO_2 in 20 rabbits (figure 1B). For the 6 remaining models, PRP gels were placed in both sides. The periosteum and skin were sutured with VICRYL l4/0 and silk 3/0, respectively, and coated with oxytetracycline.

After the follow-up period, X-ray radiography was done with an X-ray machine (Planmeca Intra, Finland) in the second, sixth, and eighth postoperative weeks. Scaffold absorption was compared through an analysis of the radiographs with respect to pixel intensity by ImageJ. (http://imagej.nih.gov/ij/index.html).

Histologic Preparation

After the muscle was stripped, the specimens were fixed in 10% formaldehyde (Sina Chemical Industrial, Iran), decalcified by 10% EDTA (pH 7.4) for about 3 months, embedded in paraffin, sectioned at a thickness of 5 μm, and stained with the hematoxylin and eosin method. Morphometric analyses were performed by ImageJ, and the percentages of the area occupied by bone and connective tissue and also the number of osteoblasts and osteocytes were estimated.
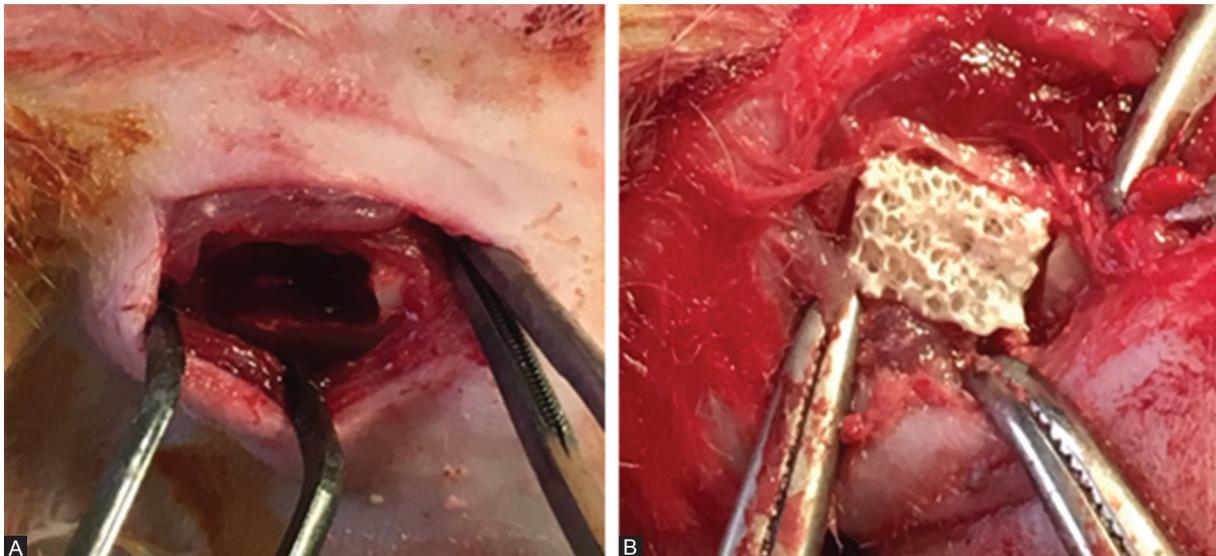
Statistical Analysis

The data were analyzed using the analysis of variance (ANOVA) to compare the difference in the mean of the percentage of the area occupied by bone and connective tissue and the number of bone cells between the 3 groups. Further analysis was done using the least significant difference (LSD) test to compare the mean value of each 2 groups. A P value less than 0.05 was considered significant. All the analyses were performed by SPSS, version 16.0, for Windows and the graph was depicted by GraphPad 5.

Results

All the rabbits tolerated the surgery and were able to eat normal diet postoperatively, but 1 rabbit was eliminated from the analysis because of the surgical site infection.

SEM

The examination of the scaffolds with SEM revealed good porosity in the HA/ZrO_2 scaffold. The pores were filled well with the PRP gel in the $HA/ZrO_2/PRP$ scaffold. The higher magnification of the PRP scaffolds exhibited nanoscale porosity. Some platelets were found within the scaffolds (figure 2).

Figure 1: Rectangular bone defects are created in the body of the rabbit mandible (A). Scaffolds are inserted in the defects (B).

Gross Examination

At the second week, light new bone formation at the peripheries of the scaffold started in the HA/ZrO$_2$/PRP-treated group and, to a lesser extent, in the HA/ZrO$_2$-treated group. In the PRP-treated animals, the initiation of bone formation was seen at the defect margins.
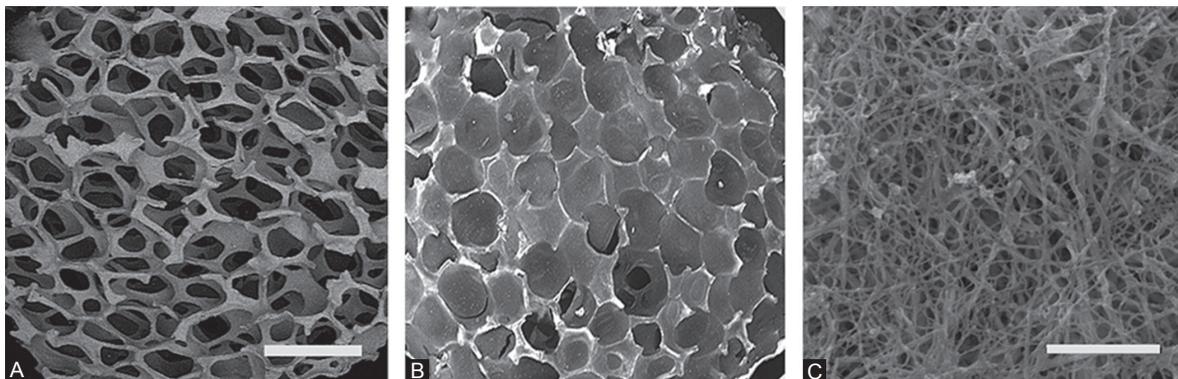
At the sixth week, a reduction in the scaffold size was observed in the HA/ZrO$_2$/PRP-treated animals; however, the scaffold materials could be seen easily. In the PRP-treated animals, bone defects could be detected easily with new bone formation.

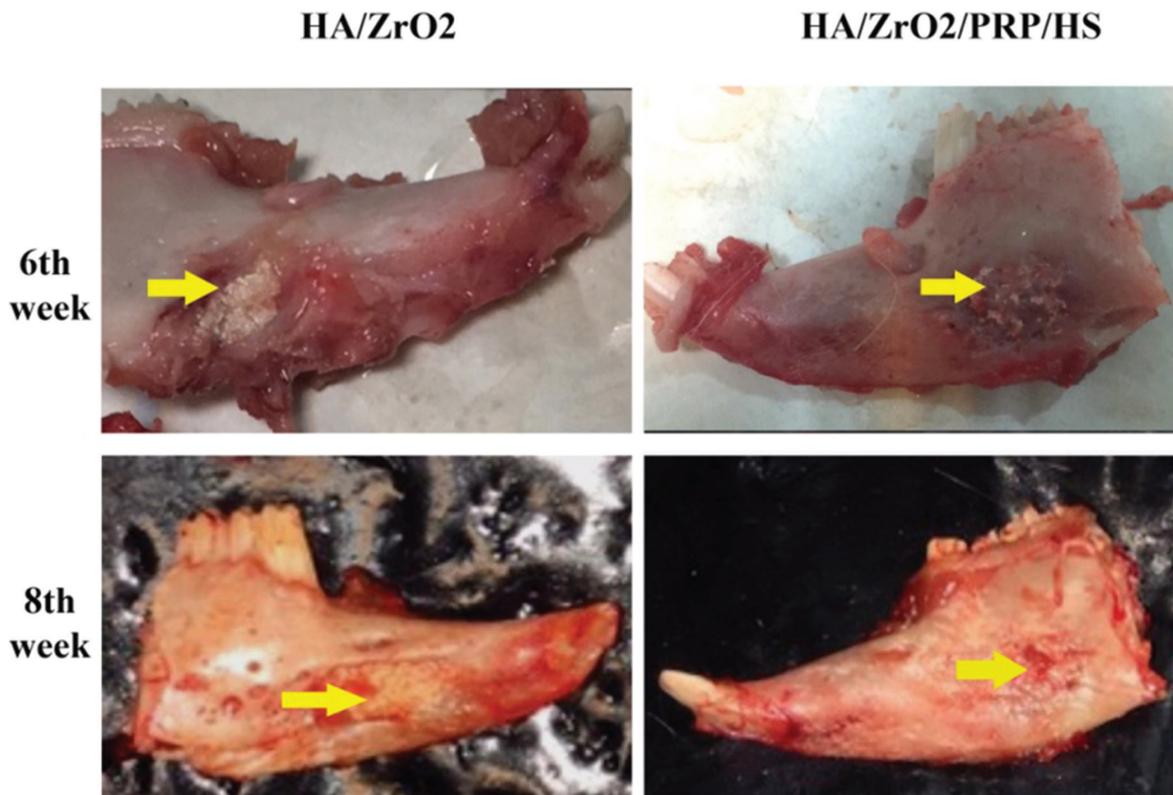At the eighth week, scaffold resorption increased and bone formation improved in both HA/ZrO$_2$/PRP- and HA/ZrO$_2$-treated groups with a slightly higher absorption in the HA/ZrO$_2$/PRP-treated rabbits (figure 3). The PRP-treated defects were partially filled with the new bone formation.
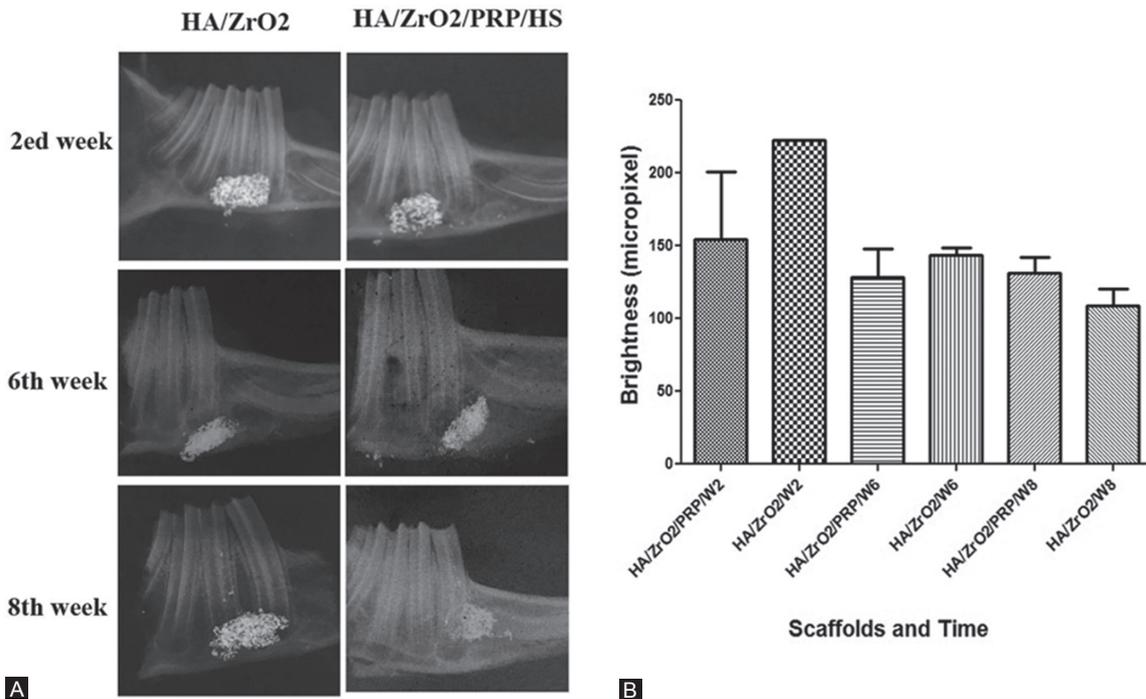
Radiologic Findings

The brightness of the scaffold area was maximum in the HA/ZrO$_2$ group at the second week, which may indicate scaffold absorption, although there was no significant difference in the pixel-intensity evaluation between HA/ZrO$_2$/PRP and HA/ZrO$_2$. Pixel-intensity evaluation also showed a nonsignificant reduction in both groups as time progressed (figure 4).

Figure 2: Scanning electron micrographs at low magnification show good porosity in the HA/ZrO$_2$ scaffold (A). Pores are also filled with PRP/HS (B). PRP scaffold contains randomly oriented fibrin fibers and platelets. It also contains nano-sized pores (C). Scale bar is 2.5 mm for A and B and 5 µm for C.

Figure 3: Gross view of the specimens at the sixth and eighth weeks shows better healing in HA/ZrO2/PRP than in HA/ZrO2.

Figure 4: Radiographs show scaffold absorption and new bone formation as the time progresses. However, analysis with ImageJ software shows that the presence of PRP does not have any significant impact on scaffold absorption. W2, Second week; W6, Sixth week; W8, Eighth week.

Histological Findings

At the second week, osteoid and woven bone appeared in both $HA/ZrO_2/PRP$- and HA/ZrO_2-treated groups, while just small islands of osteoid along with larger islands of fibrin remnant were found in the PRP-treated defects. After the specimens were decalcified, the scaffold remnant (ZrO_2) was observed as a black area. Osteoid was found in most of the cases. The estimation of the percentage of the area occupied by bone revealed a nonsignificant increase in the $HA/ZrO_2/PRP$-treated group compared with the HA/ZrO_2-treated group. According to the LSD test, the estimation of the percentage of the area occupied by bone revealed a nonsignificant increase in the $HA/ZrO_2/PRP$-treated group compared with the HA/ZrO_2-treated group and a significant increase compared with the PRP-treated defects (P=0.007). Fibrous connective tissue also predominantly filled the space between HA/ZrO_2 and newly formed woven bone in both $HA/ZrO_2/PRP$- and HA/ZrO_2-treated animals; however, a small area filled with adipose tissue was found in 50% of the cases treated with $HA/ZrO_2/PRP$ and 25% of the cases treated with HA/ZrO_2. In the PRP-treated group, 84.33%±0.2 of the total area was occupied by connective tissue containing a large number of blood vessels (figure 5).

The estimation of cell count/mm² revealed that the defects treated with $HA/ZrO_2/PRP$ contained a nonsignificantly higher number of osteocytes but a lower number of osteoblasts than those treated with HA/ZrO_2 after 2 weeks. The PRP-treated defects contained cell aggregates composed of newly differentiated osteoblasts. The newly formed osteocytes were also trapped in the osteoid. Comparing the 3 groups showed that the highest number of osteoblasts and osteocytes was present in the PRP-treated group (both Ps=0.001). No sign of inflammation was present in the histological sections of the defected bones.

At the sixth week, the percentage of the area occupied by bone increased significantly in all the groups compared with their counterparts at the second week (P=0.001 for all). Both $HA/ZrO_2/PRP$ and HA/ZrO_2 scaffolds induced woven bone along with lamellar bone and immature Haversian canal formation. A significant increase in the percentage of the area occupied by bone was also shown in the PRP-treated defects compared with the HA/ZrO_2-treated defects at this week (P=0.028). The amount of fibrous tissue also exhibited a significant reduction in both $HA/ZrO_2/PRP$- and HA/ZrO_2-treated defects compared with their counterparts at the second week (P=0.001). In the PRP-treated defects, bone cells produced extracellular matrix and, as a result, the percentage of the surface occupied by connective tissue decreased significantly compared with its counterpart at the second week (P=0.014). A large area filled with connective tissue was also estimated in the $HA/ZrO_2/PRP$-treated defects compared with the
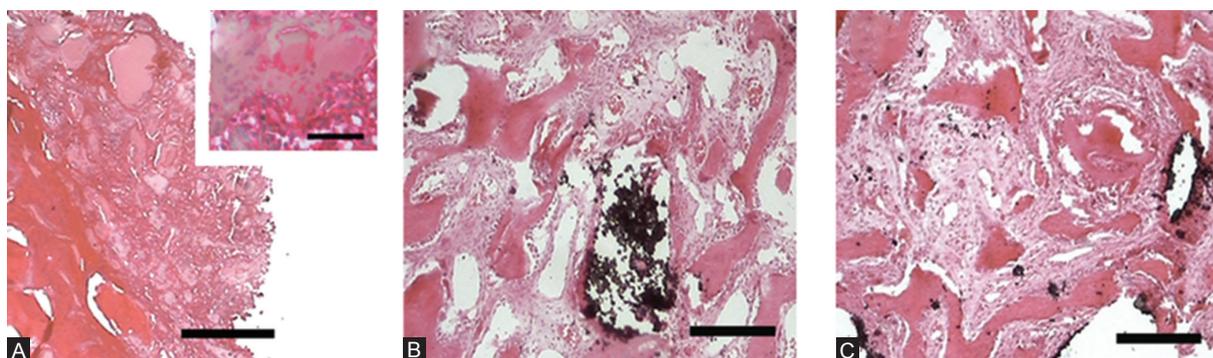
Shahsavari-Pour Sh, Aliabadi E, Latifi M, Zareifard N, Namavar MR, Talaei-Khozani T

HA/ZrO$_2$-treated defects (P=0.023). The amount of connective tissue was also significantly larger in the PRP-treated defects than in the HA/ZrO$_2$-treated defects (P=0.008). Angiogenesis was reduced in all the groups by comparison with the second week, and osteoid was hardly ever found in the cases (figure 6). The estimation of the osteoblast and osteocyte counts was the same in all the groups.

At the eighth week, a significant increase in the ossified area was detected in the HA/ZrO$_2$/PRP- and HA/ZrO$_2$-treated defects compared with their counterpart defects at the second week (P=0.0001 and P=0.025, respectively). The defects treated with HA/ZrO$_2$/PRP showed the best repair area. Connective tissue was estimated to occupy a significantly lower area in the HA/ZrO$_2$/PRP-treated defects than in the HA/ZrO$_2$- or PRP-treated defects (P=0.027 and P=0.012, respectively). Lamellar bone and Haversian canals were detected in both HA/ZrO$_2$/PRP- and HA/ZrO$_2$-treated defects but not in the PRP-treated defects (figure 7). The number of osteocytes and osteoblasts was the same in all the groups. The percentage of the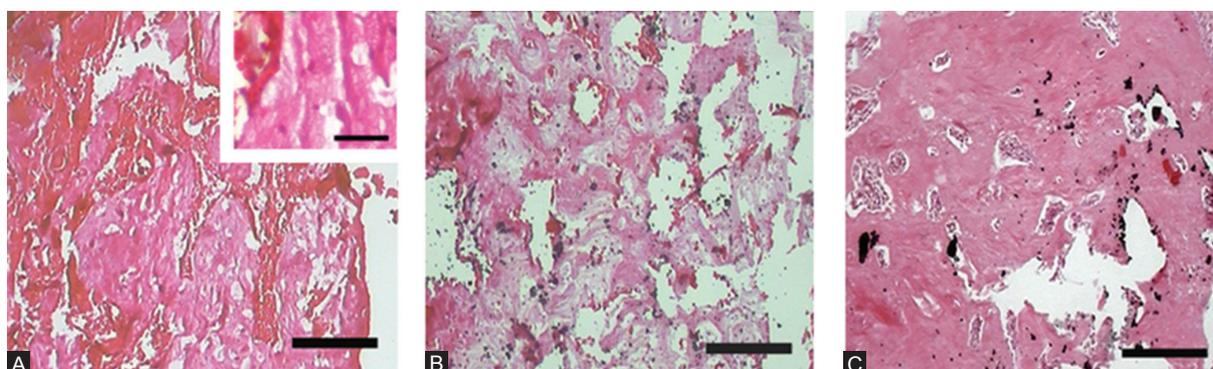 area occupied by bone and connective tissue and also the number of osteoblasts and osteocytes/mm^2 are summarized in figures 8 and 9 and table 1.
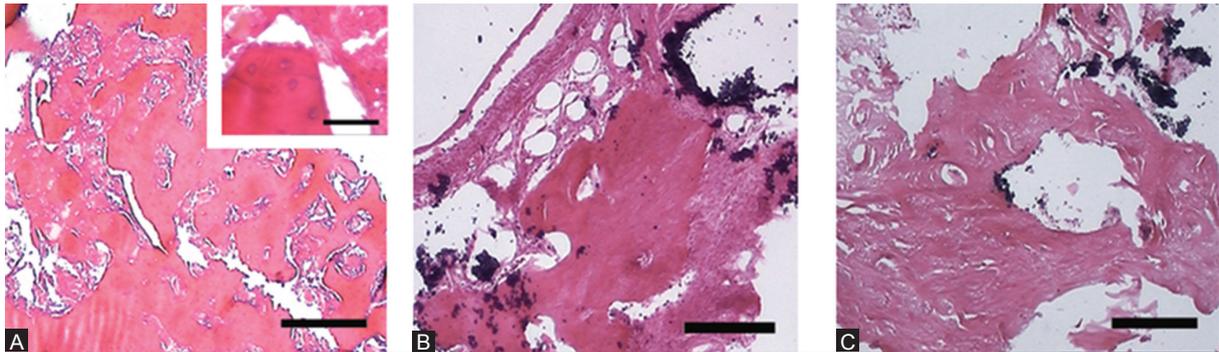
Discussion

Our data showed that PRP incorporation within a prefabricated 3D bioceramic scaffold had no significant synergic impact on bone regeneration; however, the percentage of the area occupied by connective tissue decreased in the HA/ZrO$_2$/PRP-treated defects. Although both bioceramic and PRP have osteogenic properties,[21] there are contradictory reports regarding the effectiveness of such a combination in bone regeneration. Soaking HA with PRP enhances cell activity involved in bone regeneration.[21] Also, PRP provides a bridge that connects the scaffold with the defective bone and facilitates endothelial and osteoprogenitor cell migration.[22] HA has the ability to absorb proteins temporarily and release them gradually.[23] The HA/PRP composite has been reported to increase the vertebral union in the rat lumbar interbody fusion model.[19] Further, it has been suggested that autologous bone with PRP can enhance bone formation in the rabbit defective calvaria.[24] In contrast, lack of efficiency
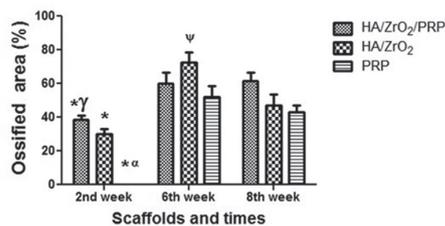

Figure 5: Micrographs show the histological sections of the defects treated with PRP (A), HA/ZrO$_2$ (B), and HA/ZrO$_2$/PRP (C) at the second week. In the PRP-treated defects, just an island of osteoid and also newly differentiated osteoblasts in the form of cell condensations (a) are present. Ossified zone with bone extracellular matrix is present in both HA/ZrO$_2$/PRP and HA/ZrO$_2$-treated defects. The black area indicates the remnant of the scaffold including ZrO$_2$. Scale bar is 200 µm for A, B, and C and 30 µm for a.

Figure 6: Micrographs show the histological sections of the defects treated with PRP (A), HA/ZrO$_2$ (B), and HA/ZrO$_2$/PRP (C) at the sixth week after surgery. Ossified zone also appears in the PRP-treated defects. However, osteoid is present in this group (a). Ossified zone with the bone extracellular matrix increases in both HA/ZrO$_2$/PRP and HA/ZrO$_2$-treated defects. Scale bar is 200 µm for A, B, and C and 30 µm for a.
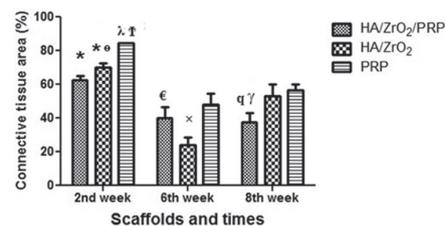
Figure 7: Micrographs show the histological sections of the defects treated with PRP (A), HA/ZrO$_2$ (B), and HA/ZrO$_2$/PRP (C) at the eighth week after surgery. Percentage of the area occupied by ossified zone also shows a significant increase in all the defect areas compared with the corresponding defects at the second week. Higher magnification of the PRP-treated defects shows that the area occupied by osteoid has decreased (a). Scale bar is 200 μm for A, B, and C and 30 μm for a.
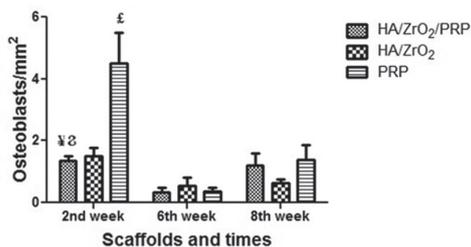

*Significant difference with their counterpart at 6th and 8th weeks (all P=0.001).

γ Significant difference with PRP-treated defects at 2nd week (P=0.007, P=0.034).

ψ Significant difference with PRP-treated at 6th weeks (P=0,028).

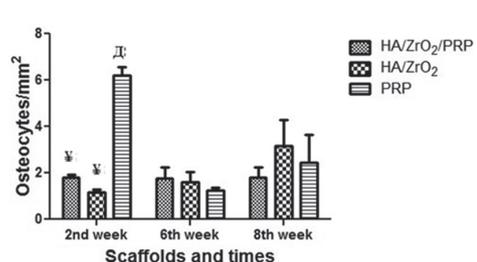α Significant difference with their counterpart at 6th week (P=0.015).

*Significant difference with their counterpart at 6th and 8th weeks (all P=0.001).

λSignificant difference with their counterpart at 6th and 8th weeks (P=0.022, P=0.046, respectively).

€ Significant difference with HA/ZrO$_2$-treated defects at 6th week (P=0.023).

q Significant difference with both HA/ZrO$_2$- and PRP-treated defects at 8th week (P=0.027, P=0.012, respectively).

ө Significant difference with HA/ZrO$_2$-treated defects at 8th week (P=0.02).

× Significant difference with PRP-treated defects at 6th week (P=0.008).

ϯ Significant difference with its counterpart at 6th and 8th week (P=0.014, 0.046).

Figure 8: Comparison of the surface occupied by bone (A) and connective tissue (B) between the HA/ZrO2/PRP-treated defects and the HA/ZrO$_2$ and PRP-treated defects.
*Significant difference with the counterpart at the sixth and eighth weeks (all Ps=0.001).
¥ Significant difference with the PRP-treated defects at the second week (P=0.007 and P=0.034).
ψ Significant difference with the PRP-treated defects at the sixth week (P=0,028).
α Significant difference with the counterpart at the sixth week (P=0.015).
€ Significant difference with the HA/ZrO2-treated defects at the sixth week (P=0.023).
q Significant difference with both HA/ZrO2- and PRP-treated defects at the eighth week (P=0.027 and P=0.012, respectively).
ө Significant difference with the HA/ZrO2-treated defects at the eighth week (P=0.02).
× Significant difference with the PRP-treated defects at the sixth week (P=0.008).
ϯ Significant difference with the counterpart at the sixth and eighth weeks (P=0.014 and P=0.046).

¥ Significant difference with PRP-treated defects at 2nd week (all P=0.001).

Ƹ Significant difference with counterparts at 6th (P=0.009, P=0.017, respectively).

£ Significant difference with all other groups (all P-0.0001).

¥ Significant difference with PRP-treated defects at 2nd week (all P=0.001).

ДSignificant difference with counterparts at 6th and 8th weeks (P=0.001, P=0.007, respectively).

Figures 9: Comparison of the number of osteoblasts (A) and osteocytes (B) between the HA/ZrO2/PRP-treated defects and the HA/ZrO$_2$ and PRP-treated defects.
¥ Significant difference with the PRP-treated defects at the second week (all Ps=0.001).
Ƹ Significant difference with the counterparts at the sixth week (P=0.009 and P=0.017, respectively).
£ Significant difference with all the other groups (all Ps=0.0001).
Д Significant difference with the counterparts at the sixth and eighth weeks (P=0.001 and P=0.007, respectively).

Table 1: Comparison of the estimated percentage of the area occupied by bone and connective tissue and estimated number of the osteoblasts and osteocytes

Groups	Weeks	Bone Area (%)±SEM	Connective Tissue Area (%)±SEM	Number of Osteocytes/mm²±SEM	Number of Osteoblasts/mm²±SEM
HA/ZrO₂/PRP	Second wk	38.388±2.868*γ	62.496±2.785λ	1.787±0.133¥	1.352±0.152¥ꝫ
	Sixth wk	59.999±6.769	40.001±6.769€	1.749±0.51	0.349±0.129¥
	Eighth wk	61.717±4.952	37.545±5.29ᑫ	1.815±0.452	1.218±0.376
HA/ZrO₂	Second wk	30.111±2.908* γ	69.889±2.908ө	1.173±0.111¥	1.495±0.267
	Sixth wk	72.409±6.127ψ	23.947±4.635×	1.613±0.428	0.550±0.267
	Eighth wk	46.849±6.7	53.151±6.7	3.361±1.116	0.649±0.105
PRP	Second wk	0.00±0.00α	84.336±0.148Ϯ	6.208±0.365Д	4.503±0.997≤
	Sixth wk	51.894±6.673	48.106±6.673	1.208±0.139	0.352±0.123
	Eighth wk	43.323±3.579	56.677±3.579	2.429±1.203	1.380±0.471

*Significant difference with the counterpart at the sixth and eighth weeks (all Ps=0.001).
γ Significant difference with the PRP-treated defects at the second week (P=0.007 and P=0.034).
ψ Significant difference with the PRP-treated defects at the sixth week (P=0.028).
α Significant difference with the counterpart at the sixth week (P=0.015).
λ Significant difference with the counterpart at the sixth and eighth weeks (P=0.022 and P=0.046, respectively).
€ Significant difference with the HA/ZrO₂-treated defects at the sixth week (P=0.023).
ᑫ Significant difference with both HA/ZrO₂- and PRP-treated defects at the eighth week (P=0.027 and P=0.012, respectively).
ө Significant difference with the HA/ZrO₂-treated defects at the eighth week (P=0.02).
× Significant difference with the PRP-treated defects at the sixth week (P=0.008).
Ϯ Significant difference with the counterpart at the sixth and eighth weeks (P=0.014 and P=0.046).
¥ Significant difference with the PRP-treated defects at the second week (all Ps=0.001).
Д Significant difference with the counterparts at the sixth and eighth weeks (P=0.001 and P=0.007, respectively).
ꝫ Significant difference with the counterparts at the sixth week (P=0.009 and P=0.017, respectively).
≤ Significant difference with all the other groups (all Ps=0.0001).

has been reported in rabbit defective maxilla regeneration with the same combination,[20] and no synergic effect has been shown by treating the rabbit vertebra with HA granules and PRP.[25] Still, there is other evidence hinting at the formation of fibrous tissue rather than bone in chitosan/gelatin/platelet/HA-treated defects in rats.[26] Our data also suggested no synergic effect of such a combination.

In the current study, both HA/ZrO₂-based scaffolds were more effective than PRP in early bone regeneration. The early stage of the healing period of the goat tibia can be improved by covering the PRP-coated titanium cylinder with calcium phosphate.[27] This finding along with our data shows that HA exerts a more beneficial effect on bone healing than the PRP gel. In contrast, the liquid form of PRP around the HA/collagen beads can induce more capillaries, osteoid, and mineralization in the rabbit iliac bone.[28] Although both PRP liquid and gel administration augment bone regeneration,[20] the liquid form is the dichotomous choice.[27]

The results of the current study also indicated high connective tissue formation in the PRP-treated defects compared with the HA/ZrO₂/PRP- or HA/ZrO₂-treated defects in the rabbit model. Osteogenic activity has been demonstrated in human PRP, but research has shown a wide variety in the PRP of different species.[29] Nevertheless, radiological findings in humans have resulted in controversy regarding the effectiveness of PRP versus HA. It has been shown that the human extracted tooth sockets filled with PRP enjoy better mineralization than those filled with HA and bioactive glass.[30] Elsewhere, a prospective study reported that PRP induced more fibrous tissue formation and less bone healing than HA.[31]

The data from the current study indicated that HA/ZrO₂/PRP accelerated fibrin remnant removal and short-term bone formation compared with the PRP-treated defects insofar as we could not observe any fibrin island in the HA/ZrO₂/PRP-treated group. It has been suggested that soaking the HA/collagen scaffold in PRP can accelerate bone-marrow formation in the rat calvarial defect model.[32] What is also deserving of note is that we found lamellar bone and Haversian system in the HA/ZrO₂/PRP-treated group. Therefore, although PRP and HA/ZrO₂ have no synergic effect in long-term bone formation, such a combination may accelerate bone maturation.

Platelets degranulate within an hour and release their GFs. The fibrin architecture also influences the rate of GF release.[33] The release of GFs can be degraded by protease.[34] Adding HS to PRP protects GFs from biodegradation and concentrates their release at the cell surface slowly.[35] Osteolysis is diminished by heparin-like glycosaminoglycan via influence on the TGF-β signaling pathway.[36] There is evidence indicating the beneficial effects of PRP supplemented with HS. Moreover, the stability of PRP GFs is not

influenced by its combination with HA-based scaffolds.[37] Our data showed that neither HA nor HS exerted a significant effect on PRP osteogenic capacity. PRP is also a rich source of angiogenic factors.[32] According to our findings, PRP induced more angiogenesis in the short term; nevertheless, in the long term, there was no difference in angiogenesis between the defects treated with or without PRP.

The data obtained from the present study showed that the highest number of osteoblasts and osteocytes/mm^2 was present in the PRP-treated defects, where osteoid and osteoblast condensations were observed after 2 weeks. A deceleration in cell migration in the PRP-treated defects may explain the presence of the higher number of bone cells in the defective area. The lag in osteogenesis may be explained by the nanoscale porosity in PRP scaffolds. In the HA/ZrO$_2$/PRP- and HA/ZrO$_2$-treated groups, osteoblast differentiation was accelerated and the production of bone-specific extracellular matrix was promoted, which was detectable with scattered cells. As a result, there was a drop in the cell count/mm^2.

An in vitro study showed that the HA/ZrO$_2$ scaffold provided an appropriate environment for cell attachment, proliferation, and differentiation. ZrO$_2$ also improved the mechanical strength of the scaffold, which is a necessary feature for the application of engineered bone replacement in the load-bearing area.[38] Radiologic and histologic evidence from the current study showed that PRP had no influence on ZrO$_2$ degradation.

Both PRP and platelet-rich fibrin have antimicrobial effects, making them appropriate autologous additives for the regeneration of infected bone injuries.[39] The data from the present study indicated the lack of any sign of inflammation in the defect site.

The current study has several limitations. First, the amount and the content of GFs in the rabbit PRP differ from those in the humans and the osteogenesis property of PRP is species-dependent.[30] Second, our findings demonstrated that HA/ZrO$_2$ and PRP had no synergic impact in the gel form; be that as it may, we might have observed the possible synergic effects of PRP and HA/ZrO$_2$ had we examined different PRP preparation procedures or different PRP sources. Third, the presence of leukocytes in PRP and the way of administration have been suggested as critical issues,[20] which may explain the contradictory results.

Conclusion

HA/ZrO$_2$ with or without PRP provided a better environment for the regeneration of the rabbit mandible defect in the short term. However, in the long term, all the scaffolds acted in the same manner apropos bone regeneration. In addition, the application of PRP may have beneficial effects vis-à-vis short-term osteoinduction and antimicrobial properties. Although this study showed that PRP and ZrO$_2$/HA had no synergistic effect, this finding may be attributed to the species, gel versus liquid administration, and the method of HA preparation rather than the ineffectiveness of such a combination.

References

1. Shanti RM, Li WJ, Nesti LJ, Wang X, Tuan RS. Adult mesenchymal stem cells: biological properties, characteristics, and applications in maxillofacial surgery. J Oral Maxillofac Surg. 2007;65:1640-7. doi: 10.1016/j.joms.2007.04.008. PubMed PMID: 17656295.

2. Goh BT, Lee S, Tideman H, Stoelinga PJ. Mandibular reconstruction in adults: a review. Int J Oral Maxillofac Surg. 2008;37:597-605. doi: 10.1016/j.ijom.2008.03.002. PubMed PMID: 18450424.

3. Prakasam M, Locs J, Salma-Ancane K, Loca D, Largeteau A, Berzina-Cimdina L. Fabrication, Properties and Applications of Dense Hydroxyapatite: A Review. J Funct Biomater. 2015;6:1099-140. doi: 10.3390/jfb6041099. PubMed PMID: 26703750; PubMed Central PMCID: PMCPMC4695913.

4. Anvari-Yazdi A, Yazdani A, Talaei-Khozani T, Kalantar M. Extraction and viability checking of various carbonated hydroxyapatite by Whartons' Jelly Mesenchymal stem cell. Sci Int. 2013;1:132-8. doi: 10.5567/

sciintl.2013.132.138.

5. Jokanovic V, Colovic B, Markovic D, Petrovic M, Soldatovic I, Antonijevic D, et al. Extraordinary biological properties of a new calcium hydroxyapatite/poly(lactide-co-glycolide)-based scaffold confirmed by in vivo investigation. Biomed Tech (Berl). 2017;62:295-306. doi: 10.1515/bmt-2015-0164. PubMed PMID: 27285125.

6. Yoshikawa H, Tamai N, Murase T, Myoui A. Interconnected porous hydroxyapatite ceramics for bone tissue engineering. J R Soc Interface. 2009;6:S341-8. doi: 10.1098/rsif.2008.0425.focus. PubMed PMID: 19106069; PubMed Central PMCID: PMCPMC2690097.

7. Oktar FN, Agathopoulos S, Ozyegin LS, Gunduz O, Demirkol N, Bozkurt Y, et al. Mechanical properties of bovine hydroxyapatite (BHA) composites doped with SiO2, MgO, Al2O3, and ZrO2. J Mater Sci Mater Med. 2007;18:2137-43. doi: 10.1007/s10856-007-3200-9. PubMed PMID: 17619958.

8. Vasconcelos C. New challenges in the sintering of HA/ZrO2 composites. Sintering of Ceramics-New Emerging Techniques: InTech; 2012. P. 179-202.

9. Curran DJ, Fleming TJ, Towler MR, Hampshire S. Mechanical properties of hydroxyapatite-zirconia compacts sintered by two different sintering methods. J Mater Sci Mater Med. 2010;21:1109-20. doi: 10.1007/s10856-009-3974-z. PubMed PMID: 20037773.

10. Mussano F, Genova T, Munaron L, Petrillo S, Erovigni F, Carossa S. Cytokine, chemokine, and growth factor profile of platelet-rich plasma. Platelets. 2016;27:467-71. doi: 10.3109/09537104.2016.1143922. PubMed PMID: 26950533.

11. Oryan A, Alidadi S, Moshiri A. Platelet-rich plasma for bone healing and regeneration. Expert Opin Biol Ther. 2016;16:213-32. doi: 10.1517/14712598.2016.1118458. PubMed PMID: 26561282.

12. Sadeghi-Ataabadi M, Mostafavi-Pour Z, Vojdani Z, Sani M, Latifi M, Talaei-Khozani T. Fabrication and characterization of platelet-rich plasma scaffolds for tissue engineering applications. Mater Sci Eng C Mater Biol Appl. 2017;71:372-80. doi: 10.1016/j.msec.2016.10.001. PubMed PMID: 27987720.

13. Vaishnavi C, Mohan B, Narayanan LL. Treatment of endodontically induced periapical lesions using hydroxyapatite, platelet-rich plasma, and a combination of both: An in vivo study. J Conserv Dent. 2011;14:140-6. doi: 10.4103/0972-0707.82614. PubMed PMID: 21814354; PubMed Central PMCID: PMCPMC3146105.

14. Casati L, Celotti F, Negri-Cesi P, Sacchi MC, Castano P, Colciago A. Platelet derived growth factor (PDGF) contained in Platelet Rich Plasma (PRP) stimulates migration of osteoblasts by reorganizing actin cytoskeleton. Cell Adh Migr. 2014;8:595-602. doi: 10.4161/19336918.2014.972785. PubMed PMID: 25482626; PubMed Central PMCID: PMCPMC4594427.

15. Creeper F, Lichanska AM, Marshall RI, Seymour GJ, Ivanovski S. The effect of platelet-rich plasma on osteoblast and periodontal ligament cell migration, proliferation and differentiation. J Periodontal Res. 2009;44:258-65. doi: 10.1111/j.1600-0765.2008.01125.x. PubMed PMID: 19210334.

16. Gdalevitch M, Kasaai B, Alam N, Dohin B, Lauzier D, Hamdy RC. The effect of heparan sulfate application on bone formation during distraction osteogenesis. PLoS One. 2013;8:e56790. doi: 10.1371/journal.pone.0056790. PubMed PMID: 23457615; PubMed Central PMCID: PMCPMC3574072.

17. Dreyfuss JL, Regatieri CV, Jarrouge TR, Cavalheiro RP, Sampaio LO, Nader HB. Heparan sulfate proteoglycans: structure, protein interactions and cell signaling. An Acad Bras Cienc. 2009;81:409-29. PubMed PMID: 19722012.

18. Fisher MC, Li Y, Seghatoleslami MR, Dealy CN, Kosher RA. Heparan sulfate proteoglycans including syndecan-3 modulate BMP activity during limb cartilage differentiation. Matrix Biol. 2006;25:27-39. doi: 10.1016/j.matbio.2005.07.008. PubMed PMID: 16226436.

19. Kamoda H, Yamashita M, Ishikawa T, Miyagi M, Arai G, Suzuki M, et al. Platelet-rich plasma combined with hydroxyapatite for lumbar interbody fusion promoted bone formation and decreased an inflammatory pain neuropeptide in rats. Spine (Phila Pa 1976). 2012;37:1727-33. doi: 10.1097/BRS.0b013e31825567b7. PubMed PMID: 22433505.

20. Butterfield KJ, Bennett J, Gronowicz G, Adams D. Effect of platelet-rich plasma with autogenous bone graft for maxillary sinus augmentation in a rabbit model. J Oral Maxillofac Surg. 2005;63:370-6. doi: 10.1016/j.joms.2004.07.017. PubMed PMID: 15742289.

21. Rodriguez IA, Growney Kalaf EA, Bowlin GL, Sell SA. Platelet-rich plasma

in bone regeneration: engineering the delivery for improved clinical efficacy. Biomed Res Int. 2014;2014:392398. doi: 10.1155/2014/392398. PubMed PMID: 25050347; PubMed Central PMCID: PMCPMC4094865.

22. El Backly RM, Zaky SH, Canciani B, Saad MM, Eweida AM, Brun F, et al. Platelet rich plasma enhances osteoconductive properties of a hydroxyapatite-beta-tricalcium phosphate scaffold (Skelite) for late healing of critical size rabbit calvarial defects. J Craniomaxillofac Surg. 2014;42:e70-9. doi: 10.1016/j.jcms.2013.06.012. PubMed PMID: 23932544.

23. Talal A, Waheed N, Al-Masri M, McKay IJ, Tanner KE, Hughes FJ. Absorption and release of protein from hydroxyapatite-polylactic acid (HA-PLA) membranes. J Dent. 2009;37:820-6. doi: 10.1016/j.jdent.2009.06.014. PubMed PMID: 19631440.

24. Nagata MJ, Melo LG, Messora MR, Bomfim SR, Fucini SE, Garcia VG, et al. Effect of platelet-rich plasma on bone healing of autogenous bone grafts in critical-size defects. J Clin Periodontol. 2009;36:775-83. doi: 10.1111/j.1600-051X.2009.01450.x. PubMed PMID: 19614722.

25. Zakaria Z, Seman CN, Buyong Z, Sharifudin MA, Zulkifly AH, Khalid KA. Histological Evaluation of Hydroxyapatite Granules with and without Platelet-Rich Plasma versus an Autologous Bone Graft: Comparative study of biomaterials used for spinal fusion in a New Zealand white rabbit model. Sultan Qaboos Univ Med J. 2016;16:e422-e9. doi: 10.18295/squmj.2016.16.04.004. PubMed PMID: 28003887; PubMed Central PMCID: PMCPMC5135452.

26. Oryan A, Alidadi S, Bigham-Sadegh A, Meimandi-Parizi A. Chitosan/gelatin/platelet gel enriched by a combination of hydroxyapatite and beta-tricalcium phosphate in healing of a radial bone defect model in rat. Int J Biol Macromol. 2017;101:630-7. doi: 10.1016/j.ijbiomac.2017.03.148. PubMed PMID: 28363647.

27. Nikolidakis D, van den Dolder J, Wolke JG, Jansen JA. Effect of platelet-rich plasma on the early bone formation around Ca-P-coated and non-coated oral implants in cortical bone. Clin Oral Implants Res. 2008;19:207-13. doi: 10.1111/j.1600-0501.2007.01456.x. PubMed PMID: 18067601.

28. Chang SH, Hsu YM, Wang YJ, Tsao YP, Tung KY, Wang TY. Fabrication of pre-determined shape of bone segment with collagen-hydroxyapatite scaffold and autogenous platelet-rich plasma. J Mater Sci Mater Med. 2009;20:23-31. doi: 10.1007/s10856-008-3507-1. PubMed PMID: 18651114.

29. van den Dolder J, Mooren R, Vloon AP, Stoelinga PJ, Jansen JA. Platelet-rich plasma: quantification of growth factor levels and the effect on growth and differentiation of rat bone marrow cells. Tissue Eng. 2006;12:3067-73. doi: 10.1089/ten.2006.12.3067. PubMed PMID: 17518622.

30. Nathani DB, Sequeira J, Rao BH. Comparison of platelet rich plasma and synthetic graft material for bone regeneration after third molar extraction. Ann Maxillofac Surg. 2015;5:213-8. doi: 10.4103/2231-0746.175762. PubMed PMID: 26981473; PubMed Central PMCID: PMCPMC4772563.

31. Dutta SR, Passi D, Singh P, Sharma S, Singh M, Srivastava D. A randomized comparative prospective study of platelet-rich plasma, platelet-rich fibrin, and hydroxyapatite as a graft material for mandibular third molar extraction socket healing. Natl J Maxillofac Surg. 2016;7:45-51. doi: 10.4103/0975-5950.196124. PubMed PMID: 28163478; PubMed Central PMCID: PMCPMC5242074.

32. Ohba S, Sumita Y, Umebayashi M, Yoshimura H, Yoshida H, Matsuda S, et al. Onlay bone augmentation on mouse calvarial bone using a hydroxyapatite/collagen composite material with total blood or platelet-rich plasma. Arch Oral Biol. 2016;61:23-7. doi: 10.1016/j.archoralbio.2015.10.012. PubMed PMID: 26492524.

33. Dohan Ehrenfest DM, Bielecki T, Jimbo R, Barbe G, Del Corso M, Inchingolo F, et al. Do the fibrin architecture and leukocyte content influence the growth factor release of platelet concentrates? An evidence-based answer comparing a pure platelet-rich plasma (P-PRP) gel and a leukocyte- and platelet-rich fibrin (L-PRF). Curr Pharm Biotechnol. 2012;13:1145-52. PubMed PMID: 21740377.

34. Dohan Ehrenfest DM, de Peppo GM, Doglioli P, Sammartino G. Slow release of growth factors and thrombospondin-1 in Choukroun's platelet-rich fibrin (PRF): a gold standard to achieve for all surgical platelet concentrates technologies. Growth Factors. 2009;27:63-9. doi: 10.1080/08977190802636713. PubMed

PMID: 19089687.

35. Zakrzewska M, Wiedlocha A, Szlachcic A, Krowarsch D, Otlewski J, Olsnes S. Increased protein stability of FGF1 can compensate for its reduced affinity for heparin. J Biol Chem. 2009;284:25388-403. doi: 10.1074/jbc.M109.001289. PubMed PMID: 19574212; PubMed Central PMCID: PMCPMC2757240.

36. Pollari S, Kakonen RS, Mohammad KS, Rissanen JP, Halleen JM, Warri A, et al. Heparin-like polysaccharides reduce osteolytic bone destruction and tumor growth in a mouse model of breast cancer bone metastasis. Mol Cancer Res. 2012;10:597-604. doi: 10.1158/1541-7786.MCR-11-0482. PubMed PMID: 22522458.

37. J A, Kuttappan S, Keyan KS, Nair MB. Evaluation of osteoinductive and endothelial differentiation potential of Platelet-Rich Plasma incorporated Gelatin-Nanohydroxyapatite Fibrous Matrix. J Biomed Mater Res B Appl Biomater. 2016;104:771-81. doi: 10.1002/jbm.b.33605. PubMed PMID: 26821772.

38. An SH, Matsumoto T, Miyajima H, Nakahira A, Kim KH, Imazato S. Porous zirconia/hydroxyapatite scaffolds for bone reconstruction. Dent Mater. 2012;28:1221-31. doi: 10.1016/j.dental.2012.09.001. PubMed PMID: 23018082.

39. Badade PS, Mahale SA, Panjwani AA, Vaidya PD, Warang AD. Antimicrobial effect of platelet-rich plasma and platelet-rich fibrin. Indian J Dent Res. 2016;27:300-4. doi: 10.4103/0970-9290.186231. PubMed PMID: 27411660.